Computational Hysteresis in Modeling Magnetic Systems

David Kinderlehrer
Ling Ma
Carnegie Mellon University

Research Report No. 94-NA-034

November 1994

Sponsors

U.S. Army Research Office
Research Triangle Park
NC 27709

National Science Foundation
1800 G Street, N.W.
Washington, DC 20550

Computational Hysteresis in Modeling Magnetic Systems

David Kinderlehrer and Ling Ma
Carnegie Mellon University, Pittsburgh, PA 15213

Abstract—**Simulations of magnetic and magnetoelastic behavior based on micromagnetic theory exhibit hysteresis. These magnetic systems have a highly nonlinear character involving short and long range fields. Computational results are presented and the role of various energetic contributions assessed and predicted using methods of contemporary nonlinear analysis.**

I. Introduction

Simulations of magnetic and magnetostrictive behavior based on micromagnetic theory and exhibiting hysteresis are presented. These magnetic systems have a highly nonlinear character involving both short range anisotropy and elastic fields and dispersive demagnetization fields. For approaches based on imposed dynamical mechanisms such as a driving force or Landau-Lifshitz-Gilbert dissipation see [1], [2] and the references therein. For static methods hysteresis is symptomatic of the way the system navigates a path through local minima of its energy space [3]. It is not sensitive to the particular method: we implement continuation based on the conjugate gradient method, although the same results were obtained by other methods (e.g., Newton's) as well. We strive to attain an efficient algorithm with careful attention dedicated to the treatment of the demagnetization energy. It is robust: computational experiments confirm that the shape of the loop is invariant over several decades of mesh refinement.

Computational results and predictions, developed using contemporary nonlinear analysis, are presented. The width of the hysteresis loop is determined analytically in a simple case as a correction to the Stoner-Wohlfarth Theory [4]. A computed magnetostriction curve illustrates the role of microstructure in the behavior of a giant magnetostrictive material [5].

II. Framework and formulation

In the micromagnetic framework, a two dimensional magnetoelastic system is subjected to an applied magnetic field. Employing the notations

$\boldsymbol{\alpha}$	magnetization
$\boldsymbol{\varepsilon}$	2×2 linear strain matrix of displacement η
$\varphi(\boldsymbol{\varepsilon}, \boldsymbol{\alpha}, x)$	stored energy
$\mathbf{H} = (H_1, 0)$	applied magnetic field
u	potential of demagnetization field,

the energy of the system occupying a region Ω may be expressed, in simplified units, in the form

$$E(\mathbf{H}, \boldsymbol{\alpha}, \eta) = \int_\Omega (\varphi(\boldsymbol{\varepsilon}, \boldsymbol{\alpha}, x) - \mathbf{H} \cdot \boldsymbol{\alpha})\, dx + \frac{1}{2} \int_{\mathbf{R}^2} |\nabla u|^2\, dx \tag{1}$$

$$\Delta u = \nabla \cdot \boldsymbol{\alpha} \chi_\Omega \text{ in } \mathbb{R}^2 \text{ and } |\boldsymbol{\alpha}| = 1 \text{ in } \Omega.$$

The characteristic function χ_Ω of Ω is 1 in Ω and 0 elsewhere. For the computations, $\Omega = (-L, L) \times (0, 1)$, a rectangle. φ will be specified later according to the application. The results discussed here do not include exchange energy. Simulations were also executed with small exchange contributions and they behave nearly the same as those without.

III. The computation of hysteresis

The hysteresis diagram for energy (1) is computed by continuation of minimum energy solutions with respect to increasing and decreasing the applied magnetic field along the x_1-axis. The shown curve in Fig. 1 is the overlaid graphs of computed energies vs a decreasing sequence of applied fields and an increasing sequence of applied fields respectively. Fig. 2 depicts magnetostriction in the direction of interest.

The computational domain is a rectangle $\Omega = (-L, L) \times (0, 1)$, partitioned into $N_1 \times N_2$ squares of side length $h = 2L/N_1 = 1/N_2$. The magnetization is approximated by piecewise constants on the squares, and the displacement is approximated by continuous piecewise linear functions on the triangles further divided from these squares. The minimization of energy (1) is then carried out by, e.g., the Polak-Ribière version of the conjugate gradient method, or Newton's method.

We recall the essential features of this conjugate gradient procedure. It is an optimization method which resolves the displacements and the magnetization in all the cells simultaneously. Demagnetizing fields are taken as

Manuscript received March, 31, 1994.
This work is supported by the AFOSR, the ARO, and the NSF, and by the Alfred P. Sloan Foundation under Grant No. 93-6-6. Computational resources provided by the NSF through a grant to the Pittsburgh Supercomputing Center.

functionals of the magnetization field. The result is a continuous displacement and piecewise constant strain matrix and magnetization. At each value of the imposed field H, inspection of the magnetization (and strain) distribution reveals the underlying magnetic domain structure (and the domains of elastic distortion.)

The optimization procedure requires the computation of energy and also the gradient of the energy with respect to the discrete variables. We remark that the most expensive feature of these computations is the determination of the averages of the demagnetizing field ∇u on the square cells. These are nonlocal functionals of the magnetization field α, and they are needed at each iteration of each minimization step. Our implementation is efficient [6], [7], the subsequence hysteresis computations take about 3 minutes of the CPU time at over 300 MFLOPS on the CRAY YMP–C90 at the Pittsburgh Supercomputer Center.

IV. Estimation of the Width of the Hysteresis Loop in a Magnetic System

We now show how the width of the hysteresis loop may be estimated in a paradigm case, explaining the behavior of Fig. 1. For a rigid uniaxial or cubic magnet as the field is varied along the easy axis the width of the hysteresis loop is determined as a correction to the classical Stoner-Wohlfarth value. The configuration is initially saturated and at an absolute minimum of energy, with a initial magnetization nearly equal to (1,0) everywhere in the region. It remains in an absolutely minimized state until H_1 changes sign, after which it traverses a metastable regime. The regime ends in a critical field range which is characterized by magnetization reversal in the closure domain, the boundary columns of the computational grid. This feature, that the closure domains are switched first, is the basis for estimating the width of the loop. This entails a careful treatment of the demagnetization energy by methods of functional analysis and partial differential equations [8], [9]. Elasticity is not present here so

$$\varphi = \varphi(\alpha) = \kappa(\alpha_2)^2 \text{ or } \kappa(\alpha_1\alpha_2)^2, \kappa > 0, \qquad (2)$$

where κ is the anisotropy constant. The critical field H_{cr} with $\mathbf{H} = (H_{cr}, 0)$ is determined by the criterion

$$E(\mathbf{H}, \alpha) \leq E(\mathbf{H}, \mathbf{e}_1) \text{ for all } \alpha \text{ where}$$

$$\alpha = \begin{cases} \xi, & \text{in the closure domain,} \\ \mathbf{e}_1, & \text{elsewhere,} \end{cases}$$

ξ is arbitrary, $|\xi| = 1$, and $\mathbf{e}_1 = (1,0)$. Optimizing this condition for ξ, cf. [3], gives

$$H_{cr} = \max_{\xi} \left\{ \frac{\varphi(\xi)}{1-\xi_1} - \frac{1}{1-\xi_1} \frac{1}{4h} \int_D \nabla(w+u) \cdot (\mathbf{e}_1 - \xi)\, dx \right\} \qquad (3)$$

where D is the closure domain and w is the solution of the equation $\Delta w = \frac{\partial}{\partial x_1}\chi_\Omega$ in $\mathbb{R}^2$. This may be reduced analytically to the form

$$H_{cr} = \max_{\xi} \left\{ \frac{\varphi(\xi)}{1-\xi_1} - \lambda + \frac{1}{2}(1-\xi_1) \right\} = 2\kappa - \lambda \qquad (4)$$

with the correction λ given by

$$\lambda = \int_{\{x_2 = L\}} \frac{\partial w}{\partial x_1}\, dx_2 \qquad (5)$$

The equation for w may be solved explicitly and yields the value $\lambda = 0.6$ for a 2×1 rectangle. The predicted value of H_{cr} is essentially exact in the uniaxial case and varies by less than 10% of the computed value in the cubic case, even for a grid as small as 16×8, in tests across a generation of anisotropy constants κ, cf. Table I, where the critical field for each κ is measured at the beginning of the cascade.

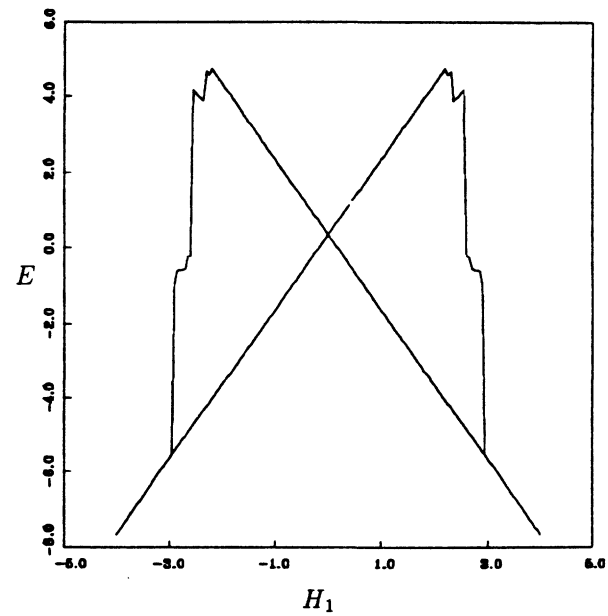

Fig. 1. Computed hysteresis picture, energy vs applied field for uniaxial materials with $\kappa = 1.6$. Units have been chosen for ease of computations.

TABLE I
Comparison of Predicted and Computed Critical Fields

κ	H_{cr} predicted	uniaxial H_{cr} computed	cubic H_{cr} computed
1.0	1.4	1.6	1.3
1.2	1.8	1.8	1.7
1.4	2.2	2.3	2.1
1.6	2.6	2.6	2.3
1.8	3.0	3.0	2.6
2.0	3.4	3.4	3.0

We remark here that a simulation with neither exchange nor demagnetization energy behaves like $N_1 \times N_2$ uncoupled cells, each with constant magnetization. They all switch at the same field value, when the magnetization becomes unstable, which is the Stoner–Wohlfarth value.

V. Magnetoelastic single crystals and laminates

Magnetostriction curves are given for single crystal and lamellar systems. The intention is to simulate Terfenol-d, a highly magnetostrictive iron/rare earth pseudobinary alloy which exhibits a complex twinned dendritic structure [10], [11]. This structure is comprised of lamella of (111) growth twins. Within each lamella, there is an array of possibly fine phase martensitic twins.

The simulation consists of a two dimensional model on an (0–11) plane and components are given with respect to axes in the (-211) and (111) directions. Anisotropy energies are

$$\varphi_{an}^{\pm}(\alpha) = \kappa(\alpha_1^2 \mp \gamma\alpha_1\alpha_2)^2, \tag{6}$$

for the single crystal φ_{an}^{+} is used, and

$$\varphi_{an}(\alpha, x) = \begin{cases} \varphi_{an}^{+} & \text{if } \frac{1}{2} < x_2 < 1, \\ \varphi_{an}^{-} & \text{if } 0 < x_2 < \frac{1}{2} \end{cases} \tag{7}$$

for the laminate where $\gamma = 2\sqrt{2}$. The magnetoelastic couplings are

$$\begin{aligned} \varphi_{el/mag}^{\pm}(\varepsilon, \alpha) &= -b(\varepsilon_{11} \mp \gamma\varepsilon_{12})(\alpha_1^2 \mp \gamma\alpha_1\alpha_2) \\ &\quad -b' \sum \varepsilon_{ij}\alpha_i\alpha_j, \end{aligned} \tag{8}$$

for the single crystal $\varphi_{el/mag}^{+}$ is used, and

$$\varphi_{el/mag}(\varepsilon, \alpha) = \begin{cases} \varphi_{el/mag}^{+} & \text{if } \frac{1}{2} < x_2 < 1, \\ \varphi_{el/mag}^{-} & \text{if } 0 < x_2 < \frac{1}{2} \end{cases} \tag{9}$$

for the laminate. For simplicity, the pure elastic energy density was chosen isotropic. For example, the easy axes for the positive energy are $(0, 1)$ and $(1, \gamma)/\sqrt{(1+\gamma^2)}$ which correspond to the directions (111) and (-111). The constants b, b', κ, and the Lamé constants are chosen for the facility of computation.

We are able to provide a qualitative comparison with experiment. The curves in Fig. 2 bear a strong resemblance to the experimental magnetostriction curve [12]. The strain increases with increasing positive and negative applied field and has the butterfly structure characteristic of this material. The *λ-jumping* described in [12] is evident in the steep section of the curve, although this is less pronounced in the experimental picture. In [12], an unbiased rod achieves about 66% of its maximum magnetostrictive strain according to the author. In our simulation we achieve about 50%. However we would like to better understand the role of growth twins and microstructure in the laminate. This is our present direction of investigation.

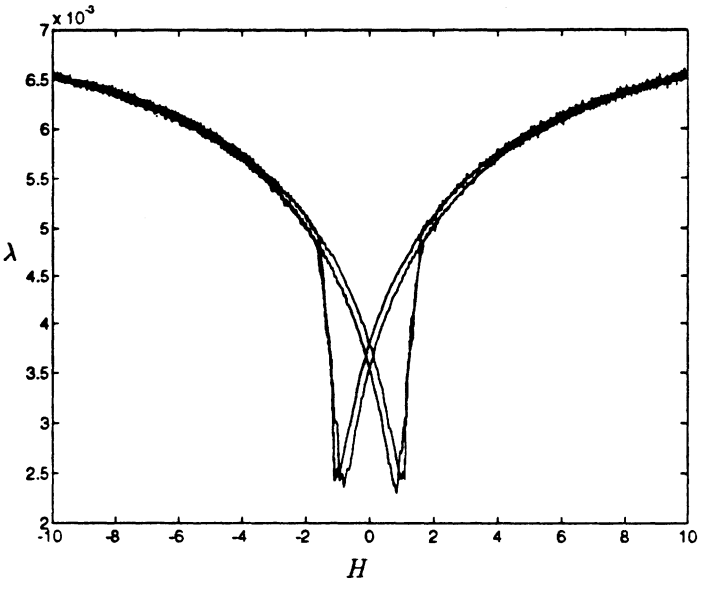

Fig. 2. Computed magnetostriction λ vs. applied field H for single crystal (lower curve) and laminate (upper curve) in the direction of the rod axis, which is (-211). Units have been chosen for ease of computation.

References

[1] R. Giles et al, "Micromagnetics of thin film cobalt-based media for magnetic recording," *Computers in Physics*, vol. 6, no. 1, 1992, pp. 53–70.

[2] D. V. Berkov et al, "Solving micromagnetic problems," *Phys. Stat. Sol.*, vol. A137, 1993, pp. 207–225.

[3] D. Kinderlehrer and L. Ma, "The hysteretic event in the computation of magnetization and magnetostriction," *Sem. Collège de France Paris*, 1994 (in press, CNA report 93-NA-031).

[4] E. C. Stoner and E. P. Wohlfarth, "A mechanism of magnetic hysteresis in heterogeneous alloys," *Phil. Trans. Roy. Soc. London*, vol. A240, 1948, pp. 599–642.

[5] R. D. James and D. Kinderlehrer, "A theory of magnetostriction with application to $TbDyFe_2$," *Phil. Mag.*, vol. B68, no. 2, 1993, pp. 237–274.

[6] M. Luskin and L. Ma, "Numerical optimization of the micromagnetics energy," *SPIE proceedings*, vol. 1919, 1993, pp. 19–29.

[7] M. Luskin and L. Ma, "Analysis of the finite element approximation of microstructure in micromagnetics," *SIAM J. Numer. Anal.*, vol. 29, no. 2, April 1992, pp. 320–331.

[8] N. I. Muskhelishvili, *Singular Integral Equations*, Dover, 1992, pp. 42–84.

[9] H. Brezis, *Analyse Fonctionnelle: Théorie et Applications*, 2e tirage, Masson, Paris, 1983.

[10] Al-Jiboory and D. Lord, *IEEE. Trans. Magn.*, vol. 26, 1990, pp. 2583–2585.

[11] J. Teter et al, *J. Appl. Phys.*, vol. 69, 1991, pp. 5768–5770.

[12] A. Clark, "High power rare earth magnetostrictive materials," *Recent adv. in adaptive and sensory materials and their applications*, Technomic, 1992, pp. 387–397.